Sensitivity of stratospheric dynamics and chemistry to QBO nudging width in the chemistry-climate model WACCM

F. Hansen,[1] K. Matthes,[1] and L. J. Gray[2]

Received 8 April 2013; revised 3 September 2013; accepted 4 September 2013; published 20 September 2013.

[1] The consequences of different quasi-biennial oscillation (QBO) nudging widths on stratospheric dynamics and chemistry are analyzed by comparing two model simulations with the National Center for Atmospheric Research's Whole Atmosphere Community Climate Model (WACCM) where the width of the QBO is varied between 22° and 8.5° north and south. The sensitivity to the nudging width is strongest in Northern Hemisphere (NH) winter where the Holton-Tan effect in the polar stratosphere, i.e., stronger zonal mean winds during QBO west phases, is enhanced for the wider compared to the narrower nudging case. The differences between QBO west and east conditions for the two model experiments can be explained with differences in wave propagation, wave-mean flow interaction, and the residual circulation. In the wider nudging case, a divergence anomaly in the midlatitude upper stratosphere/lower mesosphere occurs together with an equatorward anomaly of the residual circulation. This seems to result in a strengthening of the meridional temperature gradient and hence a significant strengthening of the polar night jet (PNJ). In the narrower nudging case, these circulation changes are weaker and not statistically significant, consistent with a weaker and less significant impact on the PNJ. Chemical tracers like ozone, water vapor, and methane react accordingly. From a comparison of westerly minus easterly phase composite differences in the model to reanalysis and satellite data, we conclude that the standard WACCM configuration (QBO22) generates more realistic QBO effects in stratospheric dynamics and chemistry during NH winter. Our study also confirms the importance of the secondary mean meridional circulation associated with the QBO for the Holton-Tan effect.

Citation: Hansen, F., K. Matthes, and L. J. Gray (2013), Sensitivity of stratospheric dynamics and chemistry to QBO nudging width in the chemistry-climate model WACCM, *J. Geophys. Res. Atmos.*, *118*, 10,464–10,474, doi:10.1002/jgrd.50812.

1. Introduction

[2] The quasi-biennial oscillation (QBO) is the dominant mode of variability in the equatorial lower to upper stratosphere [*Baldwin et al.*, 2001]. It appears as downward propagating easterly and westerly wind regimes that alternate with a variable period around 28 months. The amplitude of the QBO is asymmetric in the westerly and easterly phases with around 20 m/s in maximum for QBO west and –30 m/s for QBO east and approximately symmetric and Gaussian about the equator with a half width of approximately 12° [*Baldwin et al.*, 2001; *Pascoe et al.*, 2005]. A secondary QBO circulation is induced in order to maintain thermal wind balance. This produces a wind anomaly in the subtropics of opposite sign to that at the equator [*Plumb and Bell*, 1982; *Gray*, 2010].

[3] Influenced by this secondary circulation, the QBO is clearly evident in the distribution of chemical constituents and trace gasses like water vapor, methane, CO, or N_2O in the tropical stratosphere. The structure of the QBO in these trace gasses is approximately symmetric about the equator but with a larger subtropical anomaly in the Northern Hemisphere [*Dunkerton*, 2001; *Schoeberl et al.*, 2008].

[4] The interannual variability of ozone is also dominated by the QBO. The respective roles of the ozone QBO in different heights have been investigated in several analyses of satellite and ground-based measurements of the ozone column [e.g., *Randel and Wu*, 1996; *Choi et al.*, 1998] and model studies [e.g., *Gray*, 2000; *Butchart et al.*, 2003; *Steinbrecht et al.*, 2006; *Tian et al.*, 2006; *Punge and Giorgetta*, 2008]. In particular, recent fully coupled chemistry models confirm the existence of a transition between the direct dynamic control of ozone below approximately 28 km and the indirect chemical control above that height. The QBO influences ozone in both of these regions [*Chipperfield et al.*, 1994].

[5] Although the QBO is defined in the tropics, it does not only influence the dynamics along the equator but also

[1]GEOMAR Helmholtz Centre for Ocean Research Kiel, Kiel, Germany.
[2]Centre for Atmospheric Sciences, Department of Atmospheric, Oceanic and Planetary Physics, University of Oxford, Oxford, UK.

Corresponding author: F. Hansen, GEOMAR Helmholtz Centre for Ocean Research Kiel, Düsternbrooker Weg 20, 24105 Kiel, Germany. (fhansen@geomar.de)

2169-897X/13/10.1002/jgrd.50812

in the extratropics and especially in the polar stratosphere. On average, the polar stratospheric vortex is colder and less disturbed in QBO west winters, while winters during QBO east phase tend to be warmer and more disturbed [*Holton and Tan*, 1980, 1982]. Holton and Tan proposed a mechanism to explain this equator-to-pole connection in winter. The so-called "Holton-Tan" mechanism involves planetary waves that can propagate into the tropical lower stratosphere during the westerly phase of the QBO since the zero wind line in the lower stratosphere, which acts as a critical surface for stationary planetary wave propagation, is positioned in the summer hemisphere. In contrast, during the QBO easterly phase, the planetary waves are guided further poleward because the zero wind line is positioned in the subtropics of the winter hemisphere and they can therefore disrupt the vortex more effectively.

[6] However, *Naoe and Shibata* [2010] and *Garfinkel et al.* [2012] have recently questioned the importance of this mechanism. In their studies they found no direct evidence for the Holton-Tan mechanism and suggested that the effect of the secondary QBO circulation may be more important for the polar QBO signal than the effect of the zero wind line. It introduces a barrier for planetary wave propagation in the middle to upper stratosphere during the easterly phase, resulting in enhanced planetary wave convergence in the polar region and therefore a more disturbed polar vortex. More recently, Watson, P. A. G. and L. J. Gray [How does the quasi-biennial oscillation affect the stratospheric polar vortex?, submitted to *Journal of Atmospheric Sciences*, 2013] noted that the typical response of the polar vortex to any sort of anomalous forcing is annular mode-like, and this makes it difficult to determine cause and effect. In reality, it is likely that the position of the zero wind line and also the secondary meridional circulation will both influence planetary wave propagation, but it is not clear which is the dominant mechanism. We try to address this question with this study.

[7] Simulating the QBO is a well-known shortcoming and one of the major challenges in modeling the middle atmosphere [e.g., *SPARC CCMVal*, 2010 report]. A growing number of climate models are able to successfully generate a spontaneous QBO [*Scaife et al.*, 2000; *Giorgetta et al.*, 2002; *Shibata and Deushi*, 2005; *Kulyamin et al.*, 2009; *Kawatani et al.*, 2010; *Anstey et al.*, 2010; *Xue et al.*, 2012]. However, there are still many general circulation models (GCMs) and chemistry-climate models (CCMs) that are not able to generate a spontaneous QBO. General reasons for this deficiency can be found in insufficient spatial resolution or problems in realistically simulating small-scale processes like tropical convection [*Scaife et al.*, 2000; *Giorgetta et al.*, 2002; *Shibata and Deushi*, 2005].

[8] In order to achieve a QBO in their simulations, models without a spontaneously generated QBO employ a "nudging" technique to relax the modeled zonal wind along the equator toward observations. However, it is not clear over what latitudinal range the nudging should be applied in order to achieve the optimum representation of the QBO impact on circulation and on tracer distributions, both of which are important factors for a good representation of stratospheric climate and chemistry. In the *SPARC CCMVal* [2010] report, the QBO nudging width ranged between 7° north and south in the ECHAM/MESSY Atmospheric Chemistry (EMAC) model to between 22° north and south in the National Center for Atmospheric Research's (NCAR) Whole Atmosphere Community Climate Model (WACCM) and even 23° north and south in the Universita degli Studi L'Aquila model. A large spread was also found between the models' representation of the QBO influence on both ozone and polar variability. For example, the EMAC model with a very narrow QBO nudging width reproduced best the tropical ozone variability, while WACCM, which nudged over a much wider latitudinal range, performed comparatively poorly in this aspect (compare with *SPARC CCMVal* [2010], Figure 8.14) but performed better in polar regions, especially in simulating the Northern Hemisphere (NH) winter jet strength [*SPARC CCMVal*, 2010, Figure 4.3] and frequency of Stratospheric Sudden Warmings. Because the different models differed not only in their nudging widths but in many other respects, it was not possible to obtain a clear understanding of whether these differences in performance of the models were directly related to the chosen width of the nudging employed.

[9] The goal of this study is therefore to investigate the impact of different QBO nudging widths on the representation of QBO temperature and circulation anomalies and their impact on trace gas distributions. The studies described above have shown that the QBO affects the stratosphere in multiple ways, through its direct control of dynamical variability in the tropics, its indirect effect on the high-latitude variability, and its influence on the distribution of ozone and other radiatively active trace gasses. It is therefore an important requirement for climate models to be able to represent its impact accurately. With our analysis, we also address the question of the mechanisms behind the polar QBO influence.

[10] *Hurwitz et al.* [2011] analyzed the sensitivity of the midwinter Arctic stratosphere to the variability of the QBO width with a simplified chemistry-climate model (version 4.5.1 of the UK Met Office Unified Model). They found that a wider QBO acts like a preferential shift toward the easterly phase of the QBO, i.e., a weaker NH polar vortex. In this study we extend their analysis using a fully coupled chemistry-climate model (WACCM) and place special emphasis on the representation of the Holton-Tan mechanism in the NH polar stratosphere.

[11] The outline of this paper is as follows: Section 2 describes the model, the QBO relaxation procedure, and the simulations. Section 3 compares the QBO in the model with reanalysis data. The QBO effects on NH stratospheric dynamics and chemistry are then tested for their sensitivity to the two different QBO relaxation widths in sections 4 and 5. Final conclusions are given and discussed in section 6.

2. Model Description

[12] The model used in this study is the National Center for Atmospheric Research (NCAR) Whole Atmosphere Community Climate Model, version 3.5 (WACCM3.5). WACCM is a fully interactive CCM extending from the Earth's surface to ∼145 km. It uses the physical parametrizations from the Community Atmospheric Model, version 3.5 and the finite volume dynamical core of *Lin* [2004] with

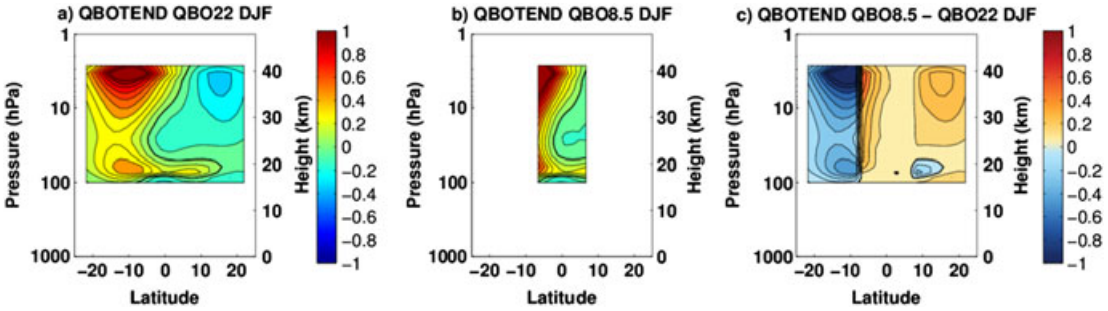

Figure 1. Wind tendency from QBO relaxation (1e-05 m/s/s) for (a) the QBO22 simulation, (b) the QBO8.5 simulation, and (c) differences between the QBO8.5 and QBO22 simulation. Contour interval 0.1 × 1e-05 m/s/s.

66 vertical levels. A detailed description of model physics specific to WACCM3 can be found in *Garcia et al.* [2007]. The changes in physical parametrization from WACCM3.1 to WACCM3.5 are described by *Richter et al.* [2010]. They mainly include changes in parametrization of convection and gravity wave drag which influences, e.g., the occurrence of sudden stratospheric warmings which are more realistic in the version used here.

[13] The horizontal resolution for the WACCM3.5 runs presented here is 1.9° × 2.5° (latitude × longitude). WACCM3.5 includes a detailed neutral chemistry scheme for the middle atmosphere based on the Model for Ozone and Related Tracers, version 3. The species included in this mechanism are contained within the O_x, NO_x, HO_x, ClO_x, and BrO_x chemical families, along with CH_4 and its degradation products [*Kinnison et al.*, 2007].

[14] Like many recent GCMs, WACCM3.5 is not able to generate a realistic QBO internally but shows weak easterlies above the equator instead. Therefore, a nudging technique based on *Balachandran and Rind* [1995] is used to relax the modeled tropical winds to observations [*Matthes et al.*, 2010]. The nudging is applied using a Gaussian weighting function decaying latitudinally from the equator with a half width of 10° which is close to the observed half width of the QBO of 10°–12° [*Baldwin et al.*, 2001]. Full vertical relaxation extends from 86 to 4 hPa, which is half that strong in one model level below and above this range (100 and 2.7 hPa, respectively) and zero for all other levels. The time constant for the relaxation of the zonal mean wind is 10 days [*Matthes et al.*, 2010]. Different from the nudging procedure described in *Matthes et al.* [2010], the semiannual oscillation (SAO) is not filtered out from the observed winds in our study before the model winds are nudged toward these winds.

[15] In the following, we will focus on extratropical feedbacks to equatorial changes because our experimental design does not allow the analysis of feedback processes in the opposite direction.

[16] *Richter et al.* [2008] found that WACCM generally exhibits a realistic middle atmosphere mean state and variability compared to observations. The most prominent model bias is an overestimation in the Southern Hemisphere (SH) polar stratospheric jet strength, which is also a common bias in other models [*SPARC CCMVal*, 2010]. Note that the frequency of stratospheric sudden warmings in the NH, an indicator of the stratospheric polar vortex variability, compares now well to ERA-40 in the model version used here (WACCM3.5) compared to WACCM version 3.1 [*Richter et al.*, 2010].

2.1. Experimental Design

[17] For this study we performed two simulations with WACCM3.5. In the first one, WACCM3.5 was run in the configuration which was also used in the SPARC CCMVal report [*SPARC CCMVal*, 2010] with the model's standard QBO nudging width extending from 22°S to 22°N and a height range of 86 to 4 hPa [*Matthes et al.*, 2010], called QBO22 hereafter. For the second simulation, called QBO8.5 hereafter, the QBO nudging width was reduced in latitudinal extend from 8.5°S to 8.5°N while the vertical range remained unchanged. The narrower nudging width of 8.5° was chosen as the closest poleward model latitude to 7°, the nudging width for the EMAC model (the model with the narrowest QBO nudging) in *SPARC CCMVal* [2010].

[18] Both simulations follow the SPARC CCMVal REF-B1 scenario [*SPARC CCMVal*, 2010] which includes the daily variations of the 11 year solar cycle and monthly variations of the QBO, Sea Surface Temperatures, greenhouse gasses, and ozone-depleting substances. Volcanic eruptions were prescribed as well. In these transient simulations, all forcings are taken from observations. The experiments cover a period from the recent past (1958–2006), of which the first 2 years of spin-up have been neglected for analysis.

[19] Figure 1 shows the wind tendency from the QBO relaxation for the QBO22 and QBO8.5 experiments in their respective nudging regions for NH winter. The strongest intervention on the modeled wind takes place in the summer hemisphere, where the prevailing easterlies are forced toward smaller amplitudes. This has also been described as the "net effect of the QBO" in *Punge and Giorgetta* [2008]. The largest differences between the forcings in QBO22 and QBO8.5 occur poleward from 8.5° in the SH (or rather in the summer hemisphere in general), where the nudging is only applied in QBO22, and equatorward of 8.5° where a stronger intervention is done in QBO8.5 (Figure 1c). Within the shared nudging region in the SH, the forcing is stronger in QBO8.5 as the prevailing easterlies are stronger in this simulation, i.e., the differences to the observed winds are larger. In the winter hemisphere, the wind tendency differences between the two simulations are smaller. So we note that the two experiments are not expected to be identical

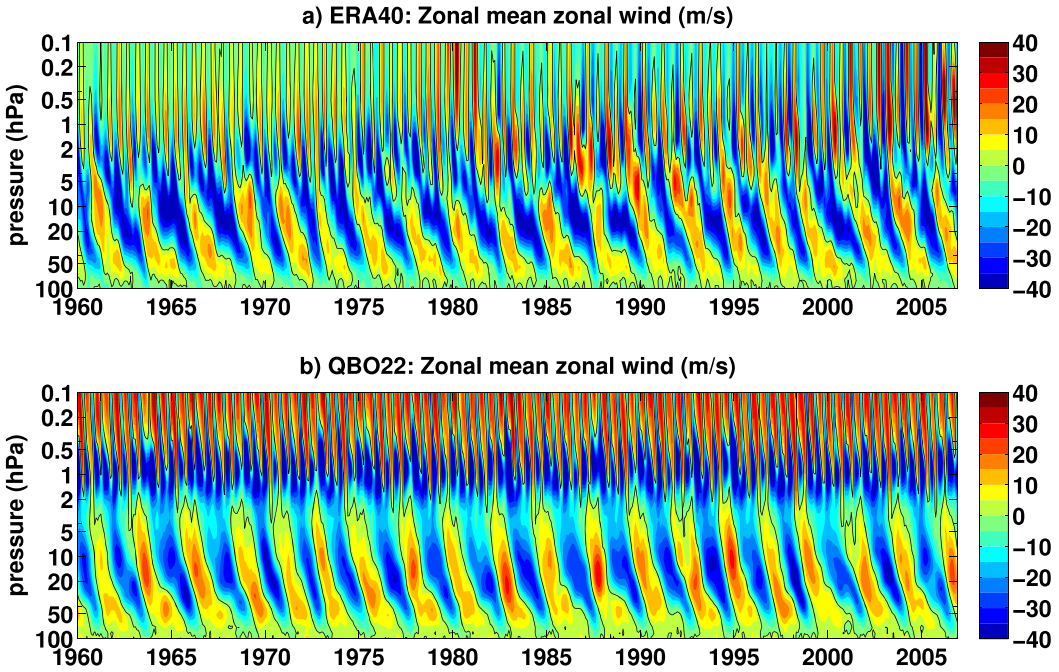

Figure 2. Zonal mean zonal wind (m/s) in the equatorial stratosphere, averaged between 2.8°S and 2.8°N, for (a) ERA-40 and (b) the QBO22 simulation, with black contour indicating the zero wind line.

above the equator, not even in the shared nudging region between 8.5° south and north.

3. QBO: Definition and Comparison Between WACCM and ERA-40

[20] As the goal of this study is to investigate WACCM's sensitivity to the width of the QBO, the next step is to compare the QBO in the model to reanalysis data. For that, the extended ERA-40 reanalysis data (abbreviated "ERA-40" in the following) are used, which means the 40 year European Centre for Medium-Range Weather Forecasts (ECMWF) Re-Analysis (ERA-40) data set [*Uppala et al.*, 2004] extended to 2008 by using the ECMWF operational analysis [*Frame and Gray*, 2010]. Different studies use different definitions for the QBO, e.g., the equatorial wind at 40 [*Baldwin et al.*, 2001; *Gray*, 2000; *Baldwin and Dunkerton*, 1998], at 44 [*Gray et al.*, 2004], or at 50 hPa and averaged over 10°S–10°N [*Yamashita et al.*, 2011] with the phases defined as positive or negative wind velocities at that level or as amplitudes more than +/– 5 m/s [*Gray*, 2000; *Gray et al.*, 2004].

[21] To differentiate between the westerly and easterly phase of the QBO, we define a QBO time series as the zonal mean zonal wind averaged between 2.8°S and 2.8°N and 43 and 51 hPa. With the resolution of WACCM3.5, this is an average over 4×2 grid points. We label a time step as QBO west phase (QBOW) when the average exceeds 5 m/s and QBO east phase (QBOE) when it falls below –2.5 m/s. The motivation for picking these particular wind thresholds is that this QBO definition turned out to be most suitable for WACCM as it leads to QBO west and east phases with approximately equal lengths.

[22] Figures 2a and 2b display the zonal mean zonal wind averaged along the equator between 2.8°S and 2.8°N for ERA-40 reanalysis data and the QBO22 simulation, respectively, for the simulated period of our experiment from 1960 to 2006. We see the expected agreement between the simulation and ERA-40 in the structure of the QBO below 10 hPa where direct wind observations exist and are assimilated in the ERA-40 data. We do not expect a perfect match between WACCM and ERA-40 for several reasons: (i) the model levels are not the same as the levels of the observations, so there might be some interpolation differences, (ii) the nudging is applied with a time constant of 10 days; this leaves some freedom to the model's resolved small-scale waves which can influence the zonal mean flow, (iii) especially in the upper part of the nudging region, the modeled SAO, which is shifted upward in WACCM as discussed in *Matthes et al.* [2010] and as can be observed in Figure 2, interacts with the SAO from the observed winds; this leads to especially QBO westerly phases reaching into higher levels compared to ERA-40, and (iv) further away from the equator, the nudging weights decay with a Gaussian function.

4. QBO Effects on Stratospheric Winter Dynamics

[23] In order to examine the effect of the QBO on tropical and extratropical dynamics in the two runs, composite differences, where QBOE composites of quantities such as zonal mean zonal wind, temperature, Eliassen-Palm (EP) flux, and residual mean meridional circulation are subtracted from QBOW composites, are computed. "Composite" thereby means the average of the quantity over all months being in the same QBO phase, e.g., QBO westerly phase for the QBOW composite. We focus the following analysis on the representation of the Holton-Tan mechanism in the northern polar winter stratosphere.

4.1. Polar Night Jet

[24] Figure 3 shows the zonal mean zonal wind differences between QBO westerly and easterly phase for Northern Hemisphere (NH) winter (December, January and February (DJF)) for the QBO22 and the QBO8.5 simulation and for ERA-40. The significance of the differences has been tested with a two-tailed Student's *t* test, and colors in Figure 3 (as in the following figures) denote that differences are statistically significant at the 95% confidence level. All figures reveal the prominent features of the equatorial QBO which is a statistically significant sandwich structure of the zonal mean zonal wind in the tropical stratosphere with a westerly wind speed anomaly of more than 20 m/s at about 40 hPa, an easterly anomaly of about 30 m/s above at about 5 hPa, and a smaller westerly anomaly of about 12 m/s above at 1 hPa. This feature is broader in QBO22 than in QBO8.5 which is a direct effect of the broader nudging along the equator in this run. Notable is also the broader extent of the easterly anomaly in height.

[25] In the extratropics, both WACCM simulations show a QBO response in the zonal mean wind which agrees with *Holton and Tan*, [1980, 1982] who showed that the polar vortex (and therefore the polar night jet (PNJ)) is stronger during QBOW phase and weaker during QBOE phase. The wind differences in the QBO22 experiment reach up to 14 m/s. That means that they are stronger and more significant at high latitudes than the wind differences in the QBO8.5 experiment which are 8 m/s at their maximum. We have also tested the statistical significance of the differences between the QBO22 and QBO8.5 responses in Figures 3a and 3b and note that the difference in response of the strength of the PNJ is significant at the 95% level, confirming that the high-latitude response is stronger in QBO22 than in QBO8.5.

[26] In ERA-40 (Figure 3c), the anomalies in the polar night reach up to 12 m/s and are statistically significant almost throughout the jet region. The PNJ anomalies in QBO8.5 are significantly weaker than in ERA-40 data, and hence, the Holton and Tan effect is more realistically reproduced in QBO22 than in QBO8.5.

4.2. Wave-Mean Flow Interactions

[27] The reasons for the nudging-dependent different responses in the PNJ can be related to differences in the propagation of planetary waves and/or its interactions with the mean flow. To analyze the origin of the zonal mean wind differences, we use the Transformed Eulerian Mean (TEM) equations [*Andrews et al.*, 1987] which describe the EP flux vector, its divergence, and the residual mean meridional circulation (meaning the meridional circulation in the TEM formalism, with v^* and w^* as its meridional and vertical components). While the EP flux vector describes the strength and propagation direction of planetary waves, its divergence describes the interaction of planetary waves with the mean flow: In a region of divergence of the EP flux vector, the mean flow is accelerated to the east, while in convergent regions, acceleration to the west occurs. Depending on the respective mean flow, this leads to a strengthening or a weakening of the circulation. During NH winter conditions with prevailing westerly background winds, a divergence (convergence) leads to acceleration (deceleration) of the flow.

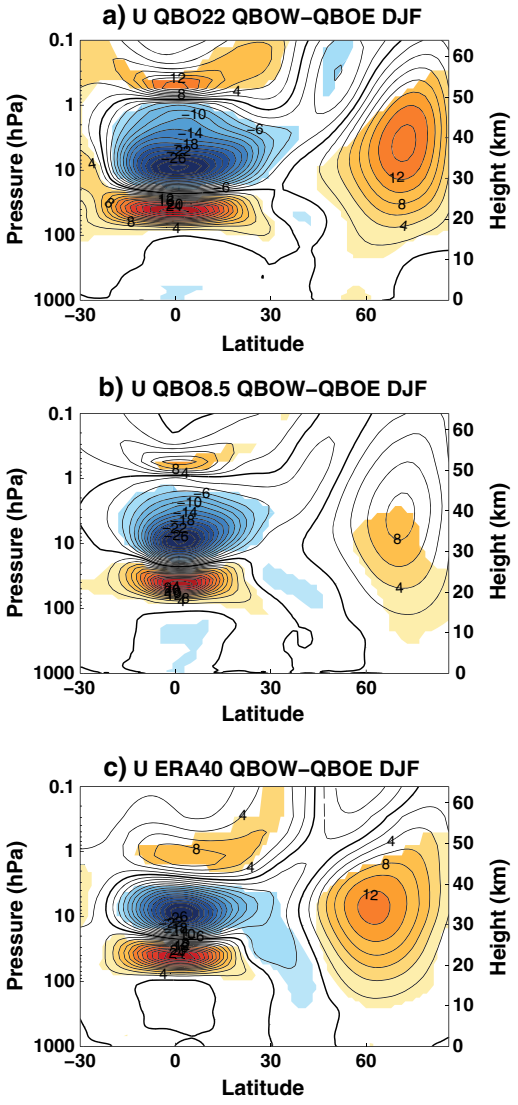

Figure 3. Differences of the zonal mean zonal wind (in m/s) between QBOW and QBOE years for (a) the QBO22, (b) the QBO8.5 experiment, and (c) ERA-40 in DJF. Contour interval: 2 m/s; color shading indicates 95% statistically significant differences.

[28] In Figure 4, vectors indicate the magnitude and direction of the EP flux vector differences between QBOW and QBOE conditions while anomalies of the EP flux vector divergence are depicted by contours. Red colors (contours and shading) mean positive (divergent) EP flux vector anomalies, and blue colors stand for negative (convergent) EP flux vector anomalies. Shaded areas highlight statistically significant differences.

[29] In Figure 4a (showing QBO22), positive EP flux divergence anomalies appear around 60°N and 0.3 hPa, i.e., exactly where we have seen the pronounced positive zonal mean wind differences in Figure 3 which indicate a strengthening of the PNJ during QBO west conditions.

[30] The zonal momentum TEM equation reveals that changes in the divergence of the EP flux vector are linked to anomalies of the residual mean circulation in the way that

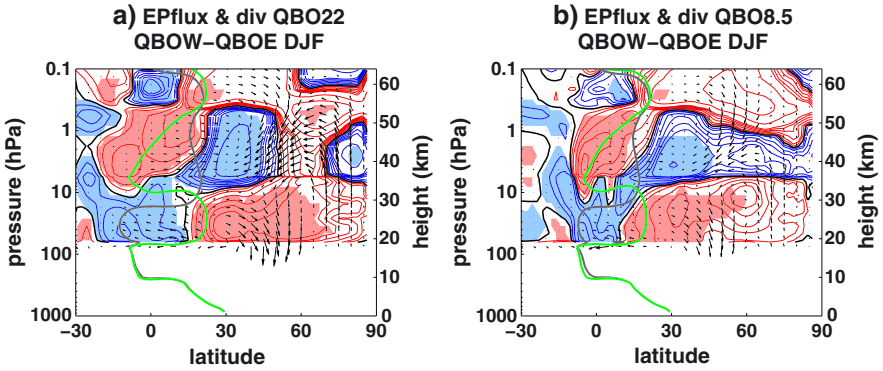

Figure 4. Differences of the EP Flux vector (arrows; scaled with the square root of pressure) and its divergence (contours; in $ms^{-1}d^{-1}$) between QBOW and QBOE years for (a) the QBO22 and (b) the QBO8.5 experiment. Contour lines: +/– 0, 0.05, 0.1, 0.2, 0.3, 0.4, 0.5, 1.0, 2.0, and 5.0 $ms^{-1}d^{-1}$; shading indicates 95% statistically significant divergence differences. The grey (green) line indicates the zero line of the zonal mean zonal wind during QBOW (QBOE) phase.

divergence leads to an equatorward anomaly of the residual circulation. This enhanced equatorward circulation can indeed be seen at around 60°N above 1 hPa in Figure 5a (for QBO22) where the QBOW–QBOE differences of the residual mean circulation are shown by vectors; the contours indicate temperature anomalies. Related to the equatorward anomaly of the residual circulation is the upward anomaly (i.e., a weakening of the prevailing net downwelling) in polar regions, especially in the upper stratosphere, together with the downward motion anomaly around 60°N, which is strongest around 1 hPa but reaches down to 10 hPa (Figure 5a for QBO22). The upward anomaly causes adiabatic cooling, while the downward anomaly leads to adiabatic warming. This together results in a strengthening of the meridional temperature gradient poleward of 60°N during QBOW as can be seen in the temperature anomaly contours in Figure 5a. The meridional temperature gradient is linked to the zonal wind by the thermal wind equation and thus is consistent with the statistically significant strengthening of the PNJ in Figure 3a.

[31] Most of the discussed features and relations can be seen in both simulations (QBO22 and QBO8.5, Figures 5a and 5b, respectively), though the response in QBO8.5 tends to be generally weaker. However, we find a major difference: In QBO8.5, there is no significant divergence anomaly in the midlatitude upper stratosphere/lower mesosphere (Figure 4b) and hence no significant effect on the residual mean circulation (Figure 5b). This is consistent with temperature anomalies that are not statistically significant throughout the PNJ region (especially not in the region of cold anomalies north of 60°N), i.e., we do not find the significant strengthening of the meridional temperature gradient which would support the significant strengthening of the jet. This implies a weaker and less statistically significant stratospheric polar vortex in QBO8.5 compared to QBO22 (Figure 3).

[32] In the tropics and NH subtropics, differences in the QBO anomalies of the EP flux vector, its divergence (Figure 4), and the residual circulation (Figure 5) between the QBO22 and QBO8.5 simulation appear only in the strength but not in the pattern of the signal. Here the anomaly patterns of the EP flux vector and its divergence involve the latitudinal position of the zero wind line which is related to the QBO (grey (QBOW) and green (QBOE) line in Figure 4). This line plays an important role for the propagation of planetary waves since these waves can

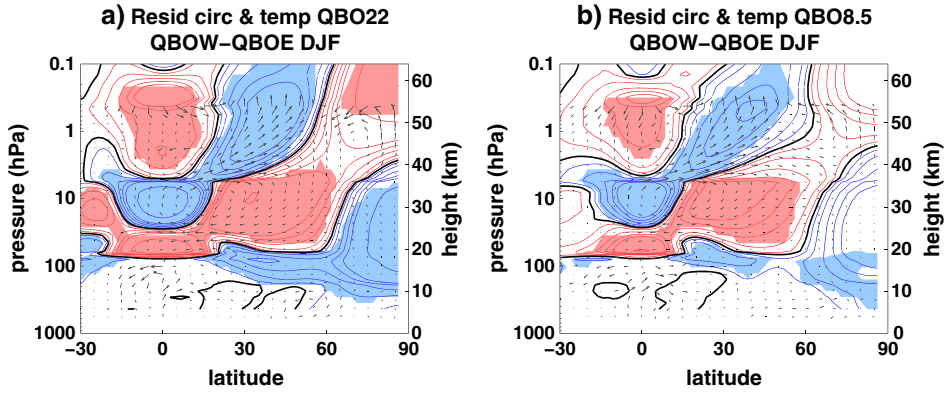

Figure 5. Same as Figure 4 but for the mean residual circulation (arrows) and temperature (contours; in °C). Contour lines: +/– 0°C, 0.2°C, 0.5°C, 1°C, 1.5°C, 2°C, 4°C, and 8°C; shading indicates 95% statistically significant temperature differences.

only propagate in (not too strong) westerly wind regimes [*Charney and Drazin*, 1961]. In the lower stratosphere around 50 hPa during QBOW, the zero wind line shifts equatorward (grey line). Planetary waves that propagate from the extratropics toward the equator can reach the equatorial lower stratosphere, whereas they are reflected to higher latitudes during QBOE (green line). Higher up in the equatorial stratosphere above 10 hPa the opposite occurs: Planetary waves propagating from the NH midlatitude troposphere toward the low-latitude upper stratosphere are restricted to the extratropics during QBOW, whereas these waves can reach the equator during QBOE, when the zero wind line is located in the Southern Hemisphere. A poleward anomaly of the EP flux vector consistent with that can be found here – in a region of consistent easterly wind anomalies seen in Figure 3 – with a divergence anomaly at the equator and a convergence anomaly around 30°N (Figure 4). The poleward anomaly of the residual mean meridional circulation (Figure 5) in the convergence anomaly region is consistent because here the converged waves lead to an enhanced wave-mean flow interaction, meaning stronger wave-induced transfer of energy and momentum to the mean flow. This reduces the mean westerly flow and, due to the disturbance of the quasi-geostrophic balance, can lead to an intensification of the poleward residual circulation in this region.

[33] In summary, our analysis suggests that the QBO nudging width in WACCM significantly influences the propagation of planetary waves as seen in the EP flux vector and its divergence as well as the residual circulation between QBO west and east years. Especially in the midlatitude upper stratosphere, differences in the divergence of the EP flux vector and hence in the residual circulation occur between QBO west and east conditions which could significantly impact meridional temperature gradient and are consistent with wind signals in the PNJ. Clear differences are seen between QBO22 and QBO8.5 reflecting the impact of the QBO nudging width on extratropical circulation.

5. QBO Effects on Chemistry

[34] Since dynamical changes like those induced by the QBO have an influence on the distribution of chemical tracers, the influence of the QBO nudging width on stratospheric chemical constituents, namely ozone and water vapor, is investigated.

[35] To see which of the WACCM simulations behaves more realistically compared to observational data, the differences between QBOW and QBOE conditions for ozone and water vapor obtained from the Global Ozone Chemistry And Related trace gas Data records for the Stratosphere (GOZCARDS) project are analyzed. GOZCARDS products are merged data sets based primarily on measurements from satellite-borne instruments and from National Aeronautics and Space Administration missions studying the Earth's stratosphere since the late 1970s. The data products used here are the ozone data set [*Wang et al.*, 2013], available from 1979 to 2012 (with the years 1981–1983 missing) in 10° latitude bins and the water vapor data set [*Anderson et al.*, 2013], available for the period 1991–2012. Since the GOZCARDS data contain fewer QBO cycles than the model data, less statistically significant results can be obtained.

5.1. Ozone

[36] The concentration of ozone in the stratosphere is a result of a combination of transport and photochemical processes. The direct impact of transport decreases with height in favor of the importance of chemical processes where the boundary between transport dominated and chemically dominated regions is often mentioned to be at 28 km (e.g., *Brasseur et al.* [1999]). While for the transport of trace species into, within, and out of the stratosphere, both the large-scale circulation and mixing processes associated with waves play a role, chemical ozone depletion not only depends on the available amount of ozone-depleting substances, but also on temperature.

[37] Figure 6 shows the differences in ozone between the QBOW and QBOE phases for the QBO22 and the QBO8.5 simulations (Figures 6a and 6b). Like for the wind anomalies, a sandwich structure is evident above the equator but only in a height range between 100 and 5 hPa in a region where the nudging has been applied, and around and below the maximum of stratospheric ozone mixing ratio at 10 hPa where the ozone concentration is dominated by transport processes. The signal peaks around 70 hPa, with an up to 30% higher ozone mixing ratio during QBOW compared to QBOE, and is quite symmetric around the equator. Additionally, a statistically significant negative ozone signal can be found in the NH polar regions around 100 hPa that extends into midlatitudes.

[38] Like for zonal wind (see previous section), the ozone differences between QBOW and QBOE conditions appear differently in the QBO22 and the QBO8.5 simulation. First, the response above the equator, i.e., the described sandwich structure, is much stronger in QBO22 than in QBO8.5, with maximum ozone differences of up to 30% compared to 20%. This is consistent with the differences between the two QBO runs in circulation (i.e., transport), concerning both strength and significance. During QBOW, the mean Brewer-Dobson circulation tropical upwelling is suppressed (Figure 4). This relative downwelling is stronger in QBO22 than in QBO8.5 which can be particularly seen in the tropical QBOW–QBOE temperature signal (Figure 5) that reaches up to 4°C in QBO22 compared to 2°C in QBO8.5.

[39] The negative polar ozone signal is strong and significant in QBO22 but very weak in the QBO8.5 run. The negative signal itself can be explained with the significantly lower temperatures during QBOW in these regions (Figure 5) which slow down the ozone production rates and also lead to more efficient ozone depletion. In addition, because of the weakened downwelling seen in the mean residual circulation signal in the polar region (Figure 5), less ozone is transported into this region. On the other hand, the negative ozone anomaly itself can also be partly responsible for the negative temperature anomaly, since ozone absorbs solar radiation and outgoing infrared radiation. Less ozone therefore means less radiation absorption and therefore lower temperatures. Both responses, in temperature and in ozone, feed back to each other. The negative temperature anomaly has been shown to be much weaker and less significant in QBO8.5 (Figure 5) which is consistent with the weaker response in ozone in this run.

[40] Differences above 5 hPa are less prominent since they are determined by the available amount of reaction

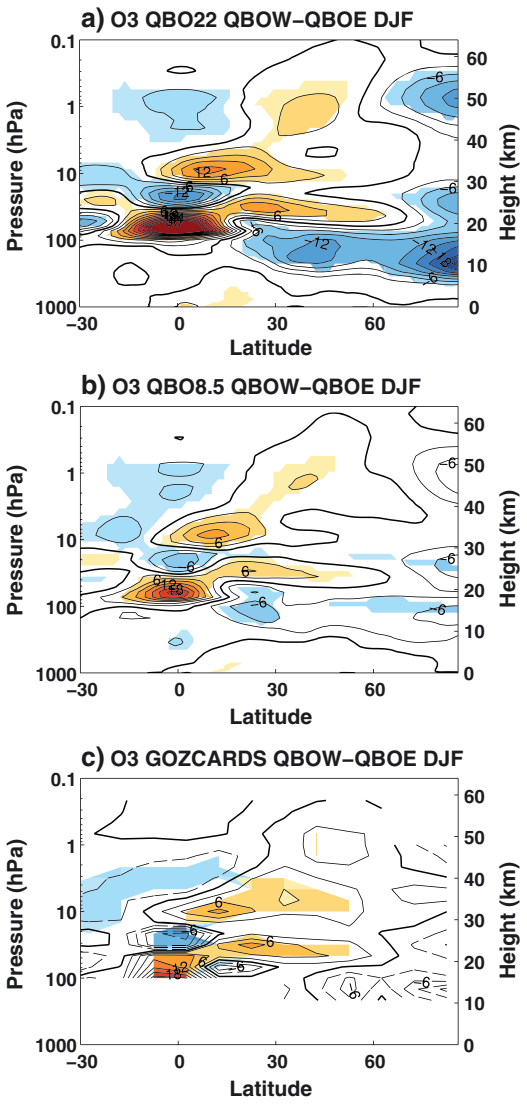

Figure 6. Differences of ozone (in %) between QBOW and QBOE years for (a) the QBO22, (b) the QBO8.5 experiment, and (c) for GOZCARDS data (1979–2012). Contour interval: 3%; color shading indicates 95% statistically significant differences.

partners for photochemical reactions (primarily NO_y (the total reactive nitrogen reservoir) [*Brasseur and Solomon*, 2005]) which are similar in both runs.

[41] Comparing our two WACCM simulations with the observed QBOW–QBOE differences from GOZCARDS (Figure 6c) reveals that the QBOW–QBOE differences above the equator are well represented in QBO8.5, while QBO22 slightly overestimates the response. In the lower stratosphere polar regions, however, it is the QBO22 experiment which outperforms the QBO8.5 simulation again, as the strength of the negative QBO signal is captured much better here. Note that due to the shorter time period of the GOZCARDS data, less statistical significances are achieved.

5.2. Water Vapor and Methane

[42] The long-lived trace gasses methane and water vapor (where "long-lived" refers to stratospheric water vapor) are transported into the lower tropical stratosphere by upwelling from the troposphere and are then transported poleward and downward by the Brewer-Dobson circulation [*Brasseur and Solomon*, 2005]. In the stratosphere, water vapor increases with height due to production via methane oxidation in this altitude [*Brasseur and Solomon*, 2005]. Therefore, the QBO response of methane and water vapor mimic each other but with opposite sign (water vapor gain = methane loss) which is why we show only the results for water vapor and discuss it where they differ from the results for methane.

[43] Figure 7 shows the difference in water vapor between the westerly and easterly QBO phase for the two WACCM experiments. In the region of the tropopause, strong positive QBO anomalies occur. These anomalies have their maximum above the equator, decrease with latitudes, and can only be seen in water vapor but not in methane. This signal can be explained with the QBO response in temperature that shows positive anomalies, i.e., higher temperatures during QBOW than QBOE, around the tropical tropopause (compare contours in Figure 5). With anomalous high temperatures, more water vapor can enter the equatorial lower stratosphere leading to the positive H_2O response at the tropical tropopause (Figure 7).

[44] Comparing now our two simulations QBO22 and QBO8.5, we mainly find differences in the strength of the signals. Especially the QBO signal of water vapor in the equatorial tropopause region is weaker in QBO8.5 than in QBO22 and restricted to a smaller latitudinal width. Furthermore, the negative anomaly above the equator around 50 hPa is almost twice as strong in QBO22 compared to QBO8.5.

[45] As it has already been observed for ozone, we find a strong QBOW–QBOE anomaly in water vapor in the NH polar lower stratosphere. It changes sign from negative (below) to positive (above) around 25 km, i.e., lies within the altitudes where water vapor concentration is dominated by transport processes. In the polar region above the tropopause, a weakened downwelling (upward anomalies) occurs in the mean residual circulation in QBOW compared to QBOE (see Figure 5) which leads to a weaker downward transport of water vapor and therefore the negative water vapor anomaly above the tropopause and the positive anomaly above. The change of sign of the signal at the pole in the stratosphere occurs exactly around the altitude of the maximum polar temperature response (also in Figure 5). The anomaly is, like for ozone, both stronger and significant in a larger region in the simulation with the wider QBO nudging.

[46] Comparing now the QBO response in WACCMs water vapor to the observed QBOW–QBOE response in GOZCARDS, we find that the structure of the signal in both constituents compares well with observations, although none of the simulations captures the strong positive anomaly above the equator around 3hPa seen in the observations. However, GOZCARDS in general shows a slightly stronger response above 50 hPa which is better represented in QBO22 than in QBO8.5.

[47] In summary for the water vapor and methane differences between the westerly and the easterly QBO phase, we find that the QBO22 run slightly better reproduces the strength of the signal but uncertainties in the observations [*Anderson et al.*, 2013] prevent firm final conclusions. The differences in water vapor and methane between the two runs are smaller than the differences seen for ozone.

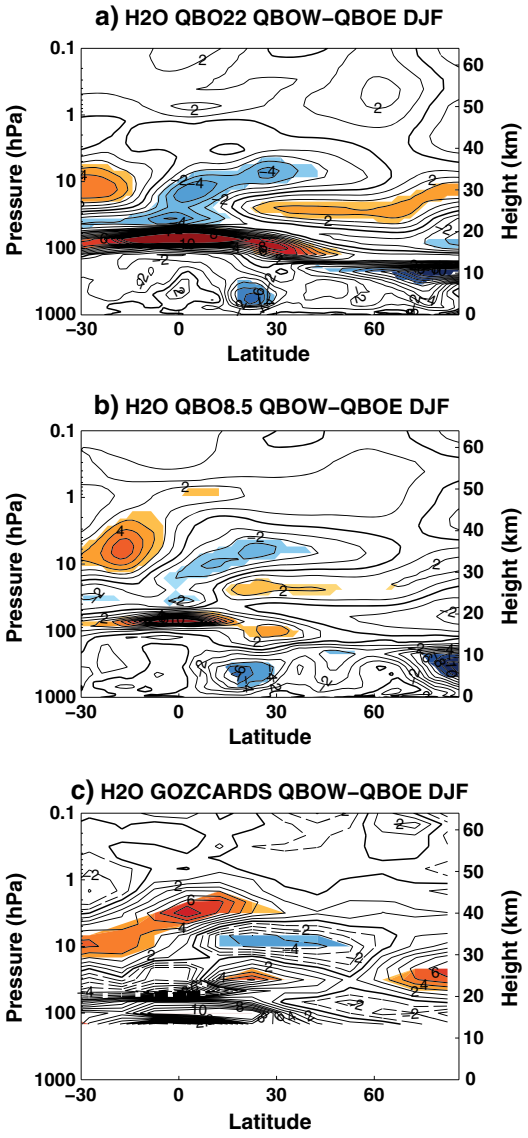

Figure 7. Same as Figure 6 but for water vapor; GOZCARDS data for 1991–2012. Contour interval: 1%; color shading indicates 95% statistically significant differences.

This confirms the findings of the SPARC CCMVal report [*SPARC CCMVal*, 2010] where WACCM was mentioned to perform very well in the stratospheric chemistry intercomparison with the exception of some deficits in representing H_2O in the polar regions.

6. Conclusions and Discussion

[48] Two 47 year simulations with the fully interactive chemistry-climate model WACCM version 3.5 were used to study the influence of the QBO nudging width on stratospheric dynamics and chemistry. For the control run, WACCM's standard QBO nudging width extending from 22°S to 22°N was used; for the second run, the latitudinal range of the wind relaxation was reduced to 8.5° south and north.

[49] The analysis of the atmospheric response to differences between QBOW and QBOE conditions in both model simulations revealed that differences in the QBO responses between the two simulations arise especially in the region of the stratospheric PNJ during NH winter (DJF). In QBO22, the zonal mean wind in the PNJ was found to be up to 14 m/s stronger during the westerly phase of the QBO than during QBOE, while the QBO response in QBO8.5 reached values only up to 8 m/s and showed less statistical significance in particular in the upper stratosphere and lower mesosphere.

[50] The connection between the equatorial QBO and the higher latitudes is consistent with the Holton-Tan mechanism, yet there are different theories on the importance of different effects: the effect of the zero wind line in the lower stratosphere which is shifted away from the equator during QBOE leading to planetary waves being reflected poleward or the effect of the secondary QBO circulation in the middle to upper stratosphere where a "barrier" to planetary wave propagation is created during QBOE in midlatitudes so that these waves converge in the polar region. From our analysis, we cannot present clear proof of the causality of this mechanism. However, dynamical arguments lead to a consistent explanation of the chain of events: In the QBO22 experiment during QBO west years, a divergence anomaly of the EP flux vector occurs around 60°N in the upper stratosphere/lower mesosphere, together with enhanced equatorward wave propagation and an equatorward anomaly of the residual mean circulation. This is consistent with a strengthening of the meridional temperature gradient in higher latitudes and hence a significant strengthening of the PNJ during QBOW. In QBO8.5, these changes in wave propagation and dissipation as well as the residual circulation are weaker than in QBO22 and not statistically significant, consistent with a weaker and less significant impact on the PNJ. Thus, our study suggests that changes in wave propagation and dissipation in the midlatitude middle to upper stratosphere associated with the equatorial QBO play a role in the modulation of the stratospheric polar vortex, similar to the findings of *Naoe and Shibata* [2010] and *Garfinkel et al.* [2012], although we note that this does not exclude a direct contribution from wave reflection at the zero wind line, as proposed originally by *Holton and Tan* [1980, 1982] [see also Watson, P. A. G. and L. J. Gray, submitted to *Journal of Atmospheric Sciences*, 2013].

[51] Consistent with the Holton and Tan response in the dynamical parameters, WACCM shows a signal in chemical tracers such as ozone, water vapor, and methane. Again, the response in QBO22 is stronger and more significant than in QBO8.5 whereupon the differences between the two experiments were larger for ozone than for water vapor and methane. The concentration and composition of these chemical constituents below 10 hPa are determined mostly by transport, while temperature-dependent chemical reactions determine the concentration and composition above that height. Therefore, the differences in chemical tracers between QBO22 and QBO8.5 in the two QBO phases are entirely consistent with the differences in the circulation and the slowing down or acceleration of the reaction velocities through changes in temperature.

[52] As a result of our investigation, we find that the optimal nudging width for WACCM is close to the model's

standard nudging width, i.e., between 22° south and north, which was also used for the *SPARC CCMVal* [2010] report. A generalization for all models can not be given within this study. When using this nudging width, the response of planetary wave propagation and the residual circulation to the forcing from the equatorial QBO agrees well with ERA-40. The QBO zonal wind response in the QBO22 run does not differ significantly from the response in ERA-40 (overestimation by +2 m/s) which reaches up to 12 m/s significantly higher wind speeds in the PNJ during QBOW compared to QBOE, whereas QBO8.5 significantly underestimates the ERA-40 response by 4 m/s. For the QBO response in chemical tracers, a comparison with GOZCARDS-merged data products confirms that the QBO22 simulation performs better than the QBO8.5 simulation keeping in mind the uncertainties in the GOZCARDS data itself. With our study we confirm a role for the mean meridional circulation associated with the QBO in influencing the polar stratospheric QBO response, although we emphasize that this does not mean that the direct mechanism proposed by *Holton and Tan* [1980, 1982] via reflection at the zero wind line is not also operating. Future studies should focus on investigating QBO effects in the recently successfully generated internal QBO in WACCM [*Xue et al.*, 2012] in order to study feedback processes between the tropical and middle to high latitudes in both directions.

[53] **Acknowledgments.** This work has been performed within the Helmholtz-University Young Investigators Group NATHAN funded by the Helmholtz-Association through the President's Initiative and Networking Fund, the Helmholtz Centre for Ocean Research Kiel (GEOMAR), the German Centre for Geosciences Potsdam (GFZ), and the Freie Universität Berlin. We thank Christopher Kadow for performing the model calculations at the Deutsche Klimarechenzentrum (DKRZ) Hamburg, Germany, and the GOZCARDS team for providing the ozone and water vapor data sets. We would like to particularly thank Chaim Garfinkel and two anonymous reviewers for their comments which helped to improve the manuscript considerably.

References

Anderson, J., L. Froidevaux, R. A. Fuller, P. F. Bernath, N. J. Livesey, H. C. Pumphrey, W. G. Read, Russell J. M. III, and K. A. Walker (2013), GOZCARDS merged data for water vapor monthly zonal means on a geodetic latitude and pressure grid, version 1.01. Greenbelt, MD, USA: NASA Goddard Earth Science Data and Information Services Center. Accessed at doi:10.5067/MEASURES/GOZCARDS/DATA3004.

Andrews, D. G., J. Holton, and C. Leovy (1987), *Middle Atmosphere Dynamics*, Academic Press, San Diego, California.

Anstey, J. A., T. G. Shepherd, and J. F. Scinocca (2010), Influence of the quasi-biennial oscillation on the extratropical winter stratosphere in an atmospheric general circulation model and in reanalysis data, *J. Atmos. Sci.*, *67*(5), 1402–1419, doi:10.1175/2009JAS3292.1.

Balachandran, N. K., and D. Rind (1995), Modeling the effects of UV variability and the QBO on the troposphere–stratosphere system. 1. The middle atmosphere, *J. Clim.*, *8*(8), 2058–2079.

Baldwin, M. P., and T. J. Dunkerton (1998), Biennial, quasi-biennial, and decadal oscillations of potential vorticity in the northern stratosphere, *J. Geophys. Res.*, *103*(D4), 3919–3928, doi:10.1029/97JD02150.

Baldwin, M. P., et al. (2001), The quasi-biennial oscillation, *Rev. Geophys.*, *39*(2), 179–229.

Brasseur, G. P., J. J. Orlando, and G. S. Tyndall (1999), *Atmospheric Chemistry and Global Change*, Oxford University Press, New York, NY, USA.

Brasseur, G. P., and S. Solomon (2005), *Aeronomy of the Middle Atmosphere: Chemistry and Physics of the Stratosphere and Mesosphere*, 3rd ed., Springer, Dordrecht, The Netherland.

Butchart, N., A. A. Scaife, J. Austin, S. H. E. Hare, and J. R. Knight (2003), Quasi-biennial oscillation in ozone in a coupled chemistry-climate model, *J. Geophys. Res.*, *108*(D15), 4486, doi:10.1029/2002JD003004.

Charney, J. G., and P. G. Drazin (1961), Propagation of planetary-scale disturbances from the lower into the upper atmosphere, *J. Geophys. Res.*, *66*, 83–109.

Chipperfield, M. P., L. J. Gray, J. S. Kinnersley, and J. Zawodny (1994), A two-dimensional model study of the QBO signal in SAGE II NO_2 and O_3, *Geophys. Res. Lett.*, *21*(7), 589–592, doi:10.1029/94GL00211.

Choi, W., W. B. Grant, J. H. Park, K. M. Lee, H. Lee, and J. M. Russell (1998), Role of the quasi-biennial oscillation in the transport of aerosols from the tropical stratospheric reservoir to midlatitudes, *J. Geophys. Res.*, *103*(D6), 6033–6042, doi:10.1029/97JD03118.

Dunkerton, T. J. (2001), Quasi-biennial and subbiennial variations of stratospheric trace constituents derived from HALOE observations, *J. Atmos. Sci.*, *58*(1), 7–25, doi:10.1175/1520-0469(2001)058<0007:QBASVO>2.0.CO;2.

Frame, T. H. A., and L. J. Gray (2010), The 11-yr solar cycle in ERA-40 data: An update to 2008, *J. Clim.*, *23*(8), 2213–2222, doi:10.1175/2009JCLI3150.1.

Garcia, R. R., D. R. Marsh, D. E. Kinnison, B. A. Boville, and F. Sassi (2007), Simulation of secular trends in the middle atmosphere, 1950–2003, *J. Geophys. Res.*, *112*, D09301, doi:10.1029/2006JD007485.

Garfinkel, C. I., T. A. Shaw, D. L. Hartmann, and D. W. Waugh (2012), Does the Holton–Tan mechanism explain how the quasi-biennial oscillation modulates the arctic polar vortex? *J. Atmos. Sci.*, *69*(5), 1713–1733, doi:10.1175/JAS-D-11-0209.1.

Giorgetta, M. A., E. Manzini, and E. Roeckner (2002), Forcing of the quasi-biennial oscillation from a broad spectrum of atmospheric waves, *Geophys. Res. Lett.*, *29*(8), 1245, doi:10.1029/2002GL014756.

Gray, L. J. (2000), A model study of the influence of the quasi-biennial oscillation on trace gas distributions in the middle and upper stratosphere, *J. Geophys. Res.*, *105*(D4), 4539–4551, doi:10.1029/1999JD900320.

Gray, L. J., S. Crooks, C. Pascoe, S. Sparrow, and M. Palmer (2004), Solar and QBO influences on the timing of stratospheric sudden warmings, *J. Atmos. Sci.*, *61*(23), 2777–2796.

Gray, L. J. (2010), Stratospheric equatorial dynamics, in The Stratosphere: Dynamics, transport, and chemistry, *Geophys. Monogr. Ser.*, *190*, 93–107.

Holton, J. R., and H.-C. Tan (1980), The influence of the equatorial quasi-biennial oscillation on the global circulation at 50 mb, *J. Atmos. Sci.*, *37*, 2200–2208.

Holton, J. R., and H.-C. Tan (1982), The quasi-biennial oscillation in the Northern Hemisphere lower stratosphere, *J. Meteorol. Soc. Jpn.*, *60*, 140–148.

Hurwitz, M. M., P. Braesicke, and J. A. Pyle (2011), Sensitivity of the mid-winter Arctic stratosphere to QBO width in a simplified chemistry-climate model, *Atmos. Sci. Lett.*, *12*, 268–272.

Kawatani, Y., K. Sato, T. J. Dunkerton, S. Watanabe, S. Miyahara, and M. Takahashi (2010), The roles of equatorial trapped waves and internal inertia-gravity waves in driving the quasi-biennial oscillation. Part I: Zonal mean wave forcing, *J. Atmos. Sci.*, *67*(4), 963–980, doi:10.1175/2009JAS3222.1.

Kinnison, D. E., et al. (2007), Sensitivity of chemical tracers to meteorological parameters in the MOZART-3 chemical transport model, *J. Geophys. Res.*, *112*, D20302, doi:10.1029/2006JD007879.

Kulyamin, D. V., E. M. Volodin, and V. P. Dymnikov (2009), Simulation of the quasi-biennial oscillations of the zonal wind in the equatorial stratosphere: Part II. Atmospheric general circulation models, *Izv. Atmos. Oceanic Phys.*, *45*(1), 37–54, doi:10.1134/S0001433809010046.

Lin, S. J. (2004), A "vertically lagrangian" finite-volume dynamical core for global models, *Mon. Weather Rev.*, *132*(10), 2293–2307, doi:10.1175/1520-0493(2004)132<2293:AVLFDC>2.0.CO;2.

Matthes, K., D. R. Marsh, R. R. Garcia, D. E. Kinnison, F. Sassi, and S. Walters (2010), Role of the QBO in modulating the influence of the 11 year solar cycle on the atmosphere using constant forcings, *J. Geophys. Res.*, *115*, D18110, doi:10.1029/2009JD013020.

Naoe, H., and K. Shibata (2010), Equatorial quasi-biennial oscillation influence on northern winter extratropical circulation, *J. Geophys. Res.*, *115*, D19102, doi:10.1029/2009JD012952.

Pascoe, C. L., L. J. Gray, S. A. Crooks, M. N. Juckes, and M. P. Baldwin (2005), The quasi-biennial oscillation: Analysis using ERA-40 data, *J. Geophys. Res.*, *110*, D08105, doi:10.1029/2004JD004941.

Plumb, R. A., and R. C. Bell (1982), A model of the quasi-biennial oscillation on an equatorial beta-plane, *Q. J. R. Meteorolog. Soc.*, *108*, 335–352.

Punge, H. J., and M. A. Giorgetta (2008), Net effect of the QBO in a chemistry climate model, *Atmos. Chem. Phys.*, *8*(21), 6505–6525.

Randel, W., and F. Wu (1996), Isolation of the ozone QBO in SAGE II data by singular-value decomposition, *J. Atmos. Sci.*, *53*, 2546–2559.

Richter, J. H., F. Sassi, and R. R. Garcia (2010), Toward a physically based gravity wave source parameterization in a general circulation model, *J. Atmos. Sci.*, *67*, 1136–156, doi:10.1175/2009JAS3112.1.

Richter, J. H., F. Sassi, R. R. Garcia, K. Matthes, and C. A. Fischer (2008), Dynamics of the middle atmosphere as simulated by the Whole Atmosphere Community Climate Model, version 3 (WACCM3), *J. Geophys. Res.*, *113*, D08101, doi:10.1029/2007JD009269.

Scaife, A. A., N. Butchart, C. D. Warner, D. Stainforth, W. Norton, and J. Austin (2000), Realistic quasi-biennial oscillations in a simulation of the global climate, *Geophys. Res. Lett.*, *27*(21), 3481–3484.

Schoeberl, M. R., et al. (2008), QBO and annual cycle variations in tropical lower stratosphere trace gases from HALOE and AURA MLS observations, *J. Geophys. Res.*, *113*, D08101, doi:10.1029/2007JD008678.

Shibata, K., and M. Deushi (2005), Partitioning between resolved wave forcing and unresolved gravity wave forcing to the quasi-biennial oscillation as revealed with a coupled chemistry-climate model, *Geophys. Res. Lett.*, *32*, L12820, doi:10.1029/2005GL022885.

SPARC CCMVal, (2010), SPARC report on the evaluation of chemistry-climate models, *SPARC-Report No. 5*, WCRP-132,WMO/TD-No. 1526, SPARC CCMVal.

Steinbrecht, W., et al. (2006), Interannual variation patterns of total ozone and lower stratospheric temperature in observations and model simulations, *Atmos. Chem. Phys.*, *6*, 349–374.

Tian, W. S., M. P. Chipperfield, L. J. Gray, and J. M. Zawodny (2006), Quasi-biennial oscillation and tracer distributions in a coupled chemistry-climate model, *J. Geophys. Res.*, *111*, D20301, doi:10.1029/2005JD006871.

Uppala, S., et al. (2004), ERA-40: ECMWF 45-year reanalysis of the global atmosphere and surface conditions 1957–2002, *ECMWF Newsletter*, *101*, 2–21.

Wang, R., L. Froidevaux, J. Anderson, R. A. Fuller, P. F. Bernath, M. P. McCormick, N. J. Livesey, J. M. Russell III, K. A. Walker, and J. M. Zawodny (2013), GOZCARDS merged data for ozone monthly zonal means on a geodetic latitude and pressure grid, version 1.01. Greenbelt, MD, USA: NASA Goddard Earth Science Data and Information Services Center. Accessed at doi:10.5067/MEASURES/GOZCARDS/DATA3006.

Xue, X. H., H. L. Liu, and X. K. Dou (2012), Parameterization of the inertial gravity waves and generation of the quasi-biennial oscillation, *J. Geophys. Res.*, *117*, D06103, doi:10.1029/2011JD016778.

Yamashita, Y., H. Akiyoshi, and M. Takahashi (2011), Dynamical response in the Northern Hemisphere midlatitude and high-latitude winter to the QBO simulated by CCSR/NIES CCM, *J. Geophys. Res.*, *116*, D06118, doi:10.1029/2010JD015016.